



Available online at www.sciencedirect.com

ScienceDirect



Nuclear Physics A 1005 (2021) 121761

www.elsevier.com/locate/nuclphysa

XXVIIIth International Conference on Ultrarelativistic Nucleus-Nucleus Collisions (Quark Matter 2019)

Flow and centrality fluctuations from ATLAS

Jiangyong Jia, on behalf of the ATLAS Collaboration

Chemistry Department, Stony Brook University, NY 11794, USA

Abstract

Results of multi-particle cumulants for harmonic flow coefficients v_n are obtained in $\sqrt{s_{\rm NN}} = 5.02$ TeV Pb+Pb collisions with the ATLAS detector at the Large Hadron Collider. The cumulant ratios $v_n\{4\}/v_n\{2\}$ for n=2,3 and 4 and $v_2\{6\}/v_2\{4\}$ show centrality-dependent behavior compatible with eccentricity fluctuations. However, significant dependences on transverse momentum are observed, suggesting that flow fluctuations may also arise from final-state interactions. The flow cumulants are also found to depend on the resolution of the quantity used to define event centrality: poorer centrality resolution tends to increase the value of $v_2\{2\}$ and changes the sign of $v_2\{4\}$ and $v_3\{4\}$ in ultra-central collisions. These results shed light on the contributions of flow fluctuations from the initial state and the final state, as well as on the influences of centrality fluctuations.

Keywords: ATLAS, heavy-ion collisions, flow fluctuations, centrality fluctuations, multi-particle cumulants

In high energy nucleus-nucleus (A+A) collisions, the distribution of produced particles exhibit strong azimuthal anisotropy as a function of transverse momentum (p_T) . Such anisotropy is analyzed with a Fourier expansion $dN/d\phi \propto 1 + 2\sum_{n=1}^{\infty} v_n \cos n(\phi - \Phi_n)$, where v_n and Φ_n represent the magnitude and angle of the n^{th} -order harmonic flow. It is well established that v_n is driven by the hydrodynamic response of the produced medium to the asymmetry in the initial-state energy density distribution, characterized by eccentricity ϵ_n , and $v_n \propto \epsilon_n$ for n = 2 and 3 [1]. The measurements of v_n and Φ_n place important constraints on the properties of the medium and on the density fluctuations in the initial state [2, 3, 4, 5].

In order to disentangle the initial- and final-state effects, experimentalists have focused their attention on flow fluctuations, $p(v_n)$. These distributions are often studied through multi-particle azimuthal correlations, $v_n\{2k\}$ [6, 7, 8], where the 2k=2,4,6... denoted the number of particles used for each multiplet. If $v_n \propto \epsilon_n$ is exact, $p(v_n)$ should be the same as $p(\epsilon_n)$ up to a rescaling factor. The latter is expected to cancel in the ratio of the cumulants such that the cumulant ratio reflects only the initial eccentricity fluctuations. On the other hand, hydrodynamic model calculations predict p_T -dependent fluctuations of v_n even in a single event [9]. Such final-state intra-event flow fluctuations may change the shape of $p(v_n)$ in a p_T -dependent way and can be quantified by comparing cumulant ratio using particles from different p_T ranges.

Another source of flow fluctuation could arise from the fact that centrality or volume of the system can not be selected precisely. Due to fluctuations in the particle production process, the true centrality for

events with the same final-state multiplicity can fluctuate from event to event. Since the v_n values vary with centrality, the centrality fluctuations (CF) is expected to influence the underlying $p(v_n)$ and the value of $v_n\{2k\}$, especially in ultra-central (UCC) collisions [10, 11].

These proceedings show multi-particle cumulants $v_n(2, 4, 6)$ for n = 2, 3, 4 obtained with the ATLAS detector [12] at the Large Hadron Collider (LHC). These results provide constraints on the $p(v_n)$, and they are compared between two centrality definitions to understand the role of CF. Results also exist for many other observables, which can be found in Ref. [13].

The flow cumulants $c_n\{2k\}$ and corresponding flow coefficients $v_n\{2k\}$ are defined as

$$\begin{split} c_n\{2\} &= \left\langle v_n^2 \right\rangle \;,\; c_n\{4\} = \left\langle v_n^4 \right\rangle - 2 \left\langle v_n^2 \right\rangle^2 \;,\; c_n\{6\} = \left\langle v_n^6 \right\rangle - 9 \left\langle v_n^4 \right\rangle \left\langle v_n^2 \right\rangle + 12 \left\langle v_n^2 \right\rangle^3 \;,\\ v_n\{2\} &= \sqrt{c_n\{2\}} \;,\; v_n\{4\} = -\mathrm{sign}(c_n\{4\}) \sqrt[4]{|c_n\{4\}|} \;,\; v_n\{6\} = \mathrm{sign}(c_n\{6\}) \sqrt[6]{\frac{1}{4}|c_n\{6\}|} \;. \end{split}$$

where $\langle v_n^{2k} \rangle$ are calculated from 2k-particle correlations [7]. The cumulant ratios (or normalized cumulants) are defined as

$$\operatorname{nc}_{n}\{4\} = \frac{c_{n}\{4\}}{c_{n}\{2\}^{2}} = -\left(v_{n}\{4\}/v_{n}\{2\}\right)^{4}, \operatorname{nc}_{n}\{6\} = \frac{c_{n}\{6\}}{4c_{n}\{2\}^{3}} = \left(v_{n}\{4\}/v_{n}\{2\}\right)^{6}. \tag{1}$$

These observables are obtained using two centrality definitions: the total transverse energy in the forward pseudorapidity range $3.2 < |\eta| < 4.9$, $\Sigma E_{\rm T}$, and the number of reconstructed charged particles in the midrapidity range $|\eta| < 2.5$, $N_{\rm ch}^{\rm rec}$. They are calculated with both the standard cumulant method [6] and the three-subevent cumulant method [14, 15, 16]. The results from the two methods are consistent, indicating that the non-flow correlations such as resonance decays and jets are not important in Pb+Pb collisions. These observables can be similarly defined for eccentricities by replacing v_n with ϵ_n , denoted by $c_n\{2k, \epsilon\}$, $v_n\{2k, \epsilon\}$ (also denoted as $\epsilon_n\{2k\}$), which describe the properties of $p(\epsilon_n)$.

Figure 1 shows the ratio of four-particle cumulants to two-particle cumulants $v_n\{4\}/v_n\{2\}$ for n=2,3 and 4. The values of $v_2\{4\}/v_2\{2\}$ increase and then decrease toward central collisions, the values of $v_3\{4\}/v_3\{2\}$ decrease continuously toward central collisions. These centrality-dependent trends are driven by the centrality dependence of the cumulants for ϵ_2 and ϵ_3 , respectively. On the other hand, significant p_T dependence is observed: the $v_2\{4\}/v_2\{2\}$ decreases for higher p_T , while $v_3\{4\}/v_3\{2\}$ shows opposite trends. Such p_T -dependences imply that the ϵ_n may not be the only source for flow fluctuations. Dynamical fluctuations in the momentum space in the initial or final state may also change $p(v_n)$.

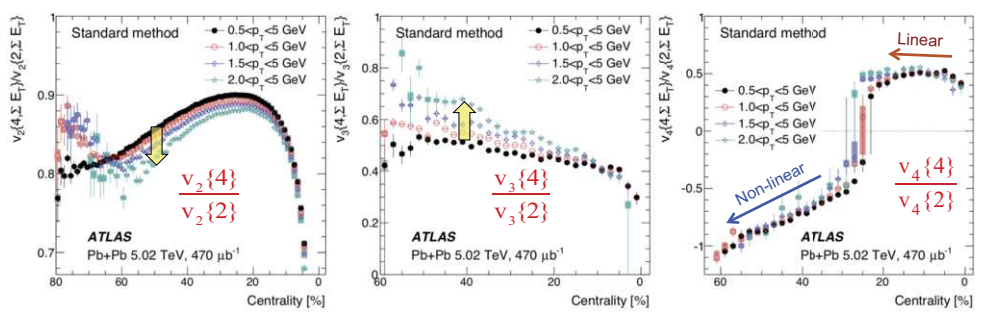


Figure 1. The centrality dependence of cumulant ratio $v_2\{4\}/v_2\{2\}$ (left), $v_3\{4\}/v_3\{2\}$ (middle), and $v_4\{4\}/v_4\{2\}$ (right) for four p_T ranges obtained from $nc_n\{4\}$ via Eq. 1 from Ref. [13]. Note that when $v_4\{4\}/v_4\{2\} < 0$, it implies $nc_4\{4\} > 0$.

Figure 1 also shows that the values of v_4 {4}/ v_4 {2} (right panel) change sign around centrality range of 25–30%. This behavior can be explained from the fact that v_4 contains a linear contribution associated with the ϵ_4 and a mode-mixing contribution from ϵ_2 due to the non-linear hydrodynamic response [17, 18]. Previous measurements [4, 5] show that the linear term dominates in central collisions, while the non-linear term dominates in more peripheral collisions.

The left panel of Figure 2 compares the cumulant ratio $v_2\{6\}/v_2\{4\}$ for $0.5 < p_T < 5$ GeV with those obtained from ALICE [19] and CMS [20] Collaborations. Excellent agreement is observed, although the

ATLAS results have much smaller statistical and systematic uncertainties. This ratio is expected to be unity for the Gaussian fluctuations, therefore the apparent deviation of the ratio from one suggests non-Gaussianity of $p(v_2)$ over a broad centrality range. Furthermore, the middle panel shows that the values of $v_2\{6\}/v_2\{4\}$ has significant p_T dependence, suggesting possible final-state contributions to flow fluctuations.

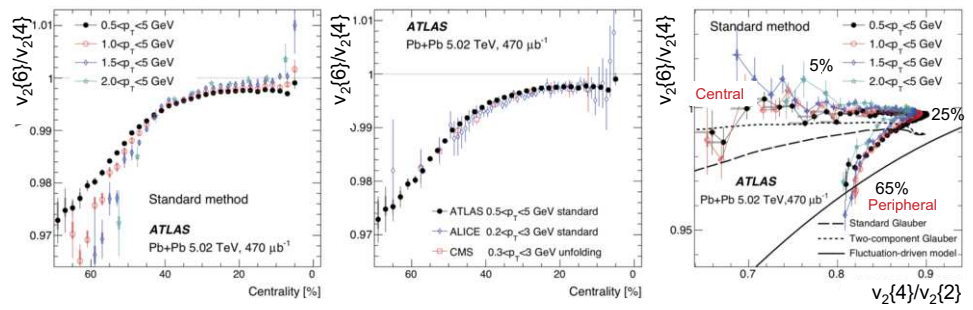


Figure 2. The centrality dependence of the cumulant ratio $v_2\{6, \Sigma E_T\}/v_2\{4, \Sigma E_T\}$ for four p_T ranges (middle) and comparison with results from ALICE Collaboration [19] and the CMS Collaboration [20] (left), and correlation between $v_2\{6, \Sigma E_T\}/v_2\{4, \Sigma E_T\}$ and $v_2\{4, \Sigma E_T\}/v_2\{2, \Sigma E_T\}$ compared with models based on initial-state eccentricities (right). From Ref. [13].

To further study $p(v_2)$ and its relation to $p(\epsilon_2)$, the right panel of Figure 2 shows the correlation between $v_2\{6\}/v_2\{4\}$ and $v_2\{4\}/v_2\{2\}$. This correlation can be compared directly to analogous correlation from elliptic eccentricity: $v_2\{6,\epsilon\}/v_2\{4,\epsilon\}$ vs $v_2\{4,\epsilon\}/v_2\{2,\epsilon\}$. The latter is calculated from three initial state models: the standard Glauber model with ϵ_2 calculated from the participating nucleons (long-dashed line) [21, 11], a two-component Glauber model with ϵ_2 calculated from a combination of participating nucleons and binary nucleon-nucleon collisions (short-dashed line) [21, 11], or a fluctuation-driven model with ϵ_2 calculated from random sources (solid line) [22]. These models fail to describe quantitatively the overall correlation pattern, although the two-component Glauber model is closest to the data in central collisions, while the fluctuation-driven model is closest to the data in peripheral collisions.

The middle panel of Figure 3 shows the correlation between $\Sigma E_{\rm T}$ and $N_{\rm ch}^{\rm rec}$. This correlation is divided into narrow intervals in either $\Sigma E_{\rm T}$ or $N_{\rm ch}^{\rm rec}$, and the mean and root-mean-square values of the $N_{\rm ch}^{\rm rec}$ ($\Sigma E_{\rm T}$) distributions are calculated and shown in the left and right panels. A linear relation is observed between $\langle N_{\rm ch}^{\rm rec} \rangle$ and $\Sigma E_{\rm T}$ over the full $\Sigma E_{\rm T}$ range, while a significant non-linear relation is observed between $\langle \Sigma E_{\rm T} \rangle$ and $N_{\rm ch}^{\rm rec}$ at large $N_{\rm ch}^{\rm rec}$. This latter behaviour suggests that, in UCC collisions, $\Sigma E_{\rm T}$ retains sensitivity to the $\langle N_{\rm ch}^{\rm rec} \rangle$ of the events, while $N_{\rm ch}^{\rm rec}$ has relatively poorer sensitivity to the $\langle \Sigma E_{\rm T} \rangle$ of the events. This implies that the true centrality is more smeared out for events with the same $N_{\rm ch}^{\rm rec}$ than those with the same $\Sigma E_{\rm T}$.

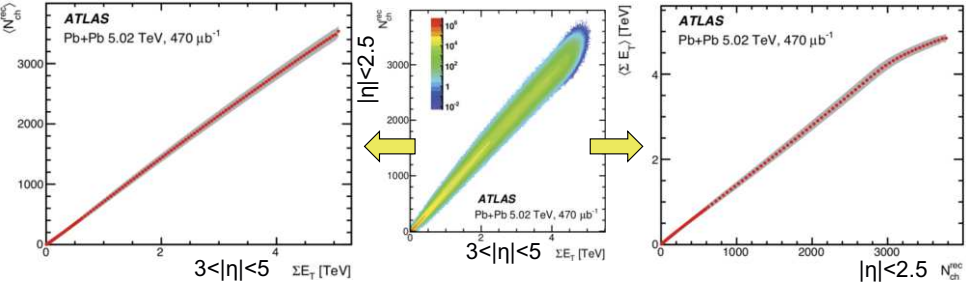


Figure 3. The correlation between N_{ch}^{rec} and ΣE_T (left), and the mean (solid points) and root-mean-square (shaded bands) of either the N_{ch}^{rec} distributions for events in slices of ΣE_T (middle) or the ΣE_T distributions for events in slices of N_{ch}^{rec} (right) from Ref. [13].

To study the influence of CF on flow fluctuations, the cumulants are measured as a function of $\langle \Sigma E_T \rangle$ or $\langle N_{\rm ch}^{\rm rec} \rangle$, denoted by $v_n\{2k, \Sigma E_T\}$ or $v_n\{2k, N_{\rm ch}^{\rm rec}\}$. They are compared to each other as a function of $\langle \Sigma E_T \rangle$ in Figure 4. The left panel shows directly the ratio $v_2\{2, N_{\rm ch}^{\rm rec}\}/v_2\{2, \Sigma E_T\}$ in two p_T ranges, which reveals a few percent deviation in the UCC region. This implies that events in a narrow $N_{\rm ch}^{\rm rec}$ range have slightly larger v_2 than events in a narrow ΣE_T , when the two ensembles have the same $\langle \Sigma E_T \rangle$, which would be the case if the

centrality resolution of $N_{\rm ch}^{\rm rec}$ was poorer than the resolution of $\Sigma E_{\rm T}$.

The middle and right panels of Figure 4 show that the values of four-particle cumulants, $nc_2\{4\}$ and $nc_3\{4\}$, also have strong sensitivity on the CF. The $nc_2\{4\}$ value changes sign in the UCC region, where it first increases, reaches a maximum and then decreases to close to zero. The $nc_3\{4\}$ value is negative and approaches zero and changes sign in the UCC region. The magnitude of the change in the UCC region is larger for $nc_n\{4, N_{ch}^{rec}\}$ than for $nc_n\{4, \Sigma E_T\}$. This behavior suggests that event class based on N_{ch}^{rec} is more affected by larger CF than event class based on ΣE_T . Such behavior is also observed for $nc_n\{4, \epsilon\}$ when the event class is defined with large CF introduced in a toy model [11].

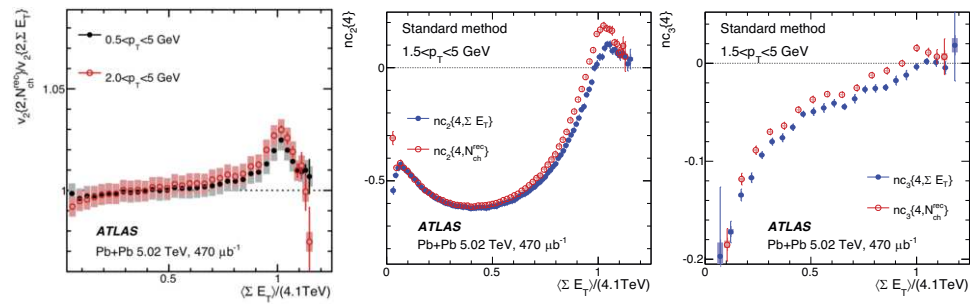


Figure 4. Comparison of flow harmonics between the two event-class definitions as a function of $\langle \Sigma E_T \rangle$ in terms of ratio $v_2\{2, N_{\rm ch}^{\rm rec}\}/v_2\{2, \Sigma E_T\}$ in two p_T ranges (left panel), $nc_2\{4, \Sigma E_T\}$ vs $nc_2\{4, N_{\rm ch}^{\rm rec}\}$ in $1.5 < p_T < 5$ GeV (middle panel) and $nc_3\{4, \Sigma E_T\}$ vs $nc_3\{4, N_{\rm ch}^{\rm rec}\}$ in $1.5 < p_T < 5$ GeV (right panel) from Ref. [13].

In summary, ATLAS has measured multi-particle cumulants for harmonic flow coefficients v_n in $\sqrt{s_{\rm NN}} = 5.02$ TeV Pb+Pb collisions at the LHC. The cumulants provide information about the event-by-event flow fluctuations and how they are affected by the centrality fluctuations. The cumulant ratios $v_n\{4\}/v_n\{2\}$ for n=2,3 and 4 and $v_2\{6\}/v_2\{4\}$ show centrality-dependent behavior compatible with eccentricity fluctuations. However significant p_T dependences are also observed, suggesting flow fluctuations may also arise directly in the momentum space through the initial-state correlations or final-state interactions. The flow cumulants also depend on the resolution for the quantity used to define event centrality: poorer centrality resolution tends to increase the value of $v_2\{2\}$ and changes the sign of $v_2\{4\}$ and $v_3\{4\}$ in ultra-central collisions.

The author acknowledges support by NSF under grant numbers PHY-1613294 and PHY-1913138.

References

- [1] D. Teaney and L. Yan, Phys. Rev. C 83 (2011) 064904, arXiv:1010.1876 [nucl-th].
- [2] ATLAS Collaboration, Phys. Rev. C 86 (2012) 014907, arXiv:1203.3087 [hep-ex].
- [3] ATLAS Collaboration, JHEP 11 (2013) 183, arXiv:1305.2942 [hep-ex].
- [4] ATLAS Collaboration, Phys. Rev. C 90 (2014) 024905, arXiv:1403.0489 [hep-ex].
- [5] ATLAS Collaboration, Phys. Rev. C **92** (2015) 034903, arXiv:1504.01289 [hep-ex].
- [6] N. Borghini, P. M. Dinh, and J.-Y. Ollitrault, Phys. Rev. C 63 (2001) 054906, arXiv:nucl-th/0007063.
- [7] A. Bilandzic, R. Snellings, and S. Voloshin, Phys. Rev. C 83 (2011) 044913, arXiv:1010.0233 [nucl-ex].
- [8] J. Jia, J. Phys. G 41 (2014) 124003, arXiv:1407.6057 [nucl-ex].
- [9] F. G. Gardim, F. Grassi, M. Luzum, and J.-Y. Ollitrault, Phys. Rev. C 87 (2013) 031901, arXiv:1211.0989 [nucl-th].
- [10] V. Skokov, B. Friman, and K. Redlich, Phys. Rev. C 88 (2013) 034911, arXiv:1205.4756 [hep-ph].
- [11] M. Zhou and J. Jia, Phys. Rev. C 98 (2018) 044903, arXiv:1803.01812 [nucl-th].
- [12] ATLAS Collaboration, JINST 3 (2008) S08003.
- [13] ATLAS Collaboration, JHEP 01 (2020) 051, arXiv:1904.04808 [nucl-ex].
- $[14] \ J.\ Jia,\ M.\ Zhou,\ and\ A.\ Trzupek,\ Phys.\ Rev.\ C\ \textbf{96}\ (2017)\ 034906,\ \texttt{arXiv:} 1701.03830\ \ [\texttt{nucl-th}].$
- [15] ATLAS Collaboration, Phys. Rev. C 97 (2018) 024904, arXiv:1708.03559 [hep-ex].
- [16] ATLAS Collaboration, Phys. Lett. B 789 (2019) 444, arXiv:1807.02012 [nucl-ex].
- $[17] \ F.\ G.\ Gardim,\ F.\ Grassi,\ M.\ Luzum,\ and\ J.-Y.\ Ollitrault,\ Phys.\ Rev.\ C\ \textbf{85}\ (2012)\ 024908,\ ar \texttt{Xiv:} 1111.6538\ [nucl-th].$
- [18] D. Teaney and L. Yan, Phys. Rev. C 86 (2012) 044908, arXiv:1206.1905 [nucl-th].
- [19] ALICE Collaboration, JHEP 07 (2018) 103, arXiv:1804.02944 [nucl-ex].
- [20] CMS Collaboration, Phys. Lett. B 789 (2019) 643, arXiv:1711.05594 [nucl-ex].
- [21] M. L. Miller, K. Reygers, S. J. Sanders, and P. Steinberg, Ann. Rev. Nucl. Part. Sci. 57 (2007) 205, arXiv:nucl-ex/0701025.
- [22] L. Yan and J.-Y. Ollitrault, Phys. Rev. Lett. 112 (2014) 082301, arXiv:1312.6555 [nucl-th].